Available online at www.sciencedirect.com
ScienceDirect
Applied Catalysis B: Environmental 72 (2007) 304–313
APPLIED CATALYSIS B: ENVIRONMENTAL
www.elsevier.com/locate/apcatb

# Gliding arc plasma assisted photocatalytic degradation of anthraquinonic acid green 25 in solution with $TiO_2$

M.R. Ghezzar, F. Abdelmalek *, M. Belhadj, N. Benderdouche, A. Addou

*Laboratoire des Sciences et Techniques de l'Environnement et de la Valorisation, Faculté des Sciences de l'Ingénieur, Université de Mostaganem 27000, Algeria*

Received 4 August 2006; received in revised form 8 November 2006; accepted 9 November 2006
Available online 14 December 2006

**Abstract**

Anthraquinonic acid green 25 (AG 25) removal was investigated by plasmachemistry using non-thermal gliding arc at atmospheric pressure. The gaseous species formed in the discharge, and especially $OH^{\bullet}$ radicals, induce strong oxidizing effects in the target solution. The removal of the dye was carried out in the absence and presence of $TiO_2$ as photocatalyst. The decolourization of AG 25 was followed by UV–vis spectrometry (at 643 nm), while the degradation was followed by COD measurements. The effects of operating variables such as initial concentration of AG 25 and catalyst concentration were investigated. Experiments were carried out to optimise the amount of $TiO_2$. The results showed that maximum degradation was attained for 2 g $L^{-1}$ $TiO_2$ concentration. At this optimum concentration, the dye (80 μM) was totally decolourized within 15 min of plasma-treatment time, and 93% removal of initial COD was attained after a 180-min plasma-treatment time. In the absence of catalyst, colour removal was 46% after 15 min, while COD abatement reached 84% after 180 min. The extent of degradation decreased with initial concentration and the time required for complete degradation increased. In all cases, the plasma-treated samples in the presence or absence of catalyst were found to follow pseudo-first order reaction kinetics. The $TiO_2$-mediated plasmachemical process showed potential application for the treatment of dye solutions, resulting in the mineralization of the dye confirmed by sulfate ion formation.


*Keywords:* Anthraquinonic dye; Degradation; Gliding arc; Plasmacatalysis; $TiO_2$

## 1. Introduction

Dye pollutants from textile industry are an important source of environmental contamination. Indeed, these effluents are often toxic, mostly non-bio-degradable and sometimes also resistant to destruction by physicochemical treatment methods. Wastewaters from textile and dye industries are characterized by strong colour, highly fluctuating pH, high chemical oxygen demand and biotoxicity [1–3]. A lot of research has recently been widely focussed on the treatment of wastewater due to more stringent international environmental standards. A number of physical, biochemical oxidation and chemical techniques had been reported for the treatment of all types of dyes, but these processes have only limited success. Biodegradation of dyes is not efficient enough due to the presence of complex and stable aromatic structures. Many different approaches have been suggested to tackle removal of dyes from aqueous solutions. Among the widely used methods are adsorption, biological degradation, coagulation processes, and ozone and hypochlorite treatments of dye waste effluents. All these methods are either costly, inefficient or result in the production of secondary waste product [4,5]. Recently, advanced oxidation processes (AOPs) have been widely investigated [6–9]. Advanced oxidation processes mainly involve the generation of a very powerful and non-selective oxidizing agent, the hydroxyl radical $OH^{\bullet}$, ($E^{\circ}_{OH^{\bullet}/H_2O} = 2.8$ V versus SHE), which can be produced by different methods. Heterogeneous catalytic oxidation processes may be by UV-induced irradiation onto $TiO_2$ [10–14] on ZnO [9], by solar photo-catalysis using $TiO_2$ and photo-Fenton processes. Among homogeneous AOPs are $UV/O_3$, $UV/H_2O_2$ and different Fenton processes like dark-Fenton, solar-Fenton

* Corresponding author. Present address: Laboratoire de Chimie Moléculaire et Environnement, ESIGEC, Université de Savoie, 73376, Le Bourget du Lac, France. Tel.: +33 4 79 75 88.36; fax: +33 4 79 75 87 72.
*E-mail address:* Fatiha.Abdelmalek@univ-savoie.fr (F. Abdelmalek).

0926-3373/$ – see front matter 
doi:10.1016/j.apcatb.2006.11.008

and UV-Fenton [15–17]. These techniques have been found especially suitable for degrading azo and anthraquinonic dyes, which are the mostly used textile colorants. Recently, gliding arc discharge has been shown to be effective at degrading organic compounds from aqueous solutions. Moreover, it is possible to perform the degradation of dye-contaminated wastewater [18,19]. In Algeria, synthetic dyes are intensely used in the textile industry activity and have serious consequences for public health. Te glidarc discharge belongs to the group of non-thermal plasmas, although it is formed from an electric arc. The nature of the activated species depends on that of the gas used. The activated species are atoms (O), radicals ($OH^{\bullet}$) or excited molecules (singlet oxygen $O_2{}^1\Delta g$). In the latter case, a modified electron distribution induces a modified and usually enhanced reactivity. Emission spectroscopy measurements on gliding arc plasma in humid air revealed the simultaneous presence of $OH^{\bullet}$ and $NO^{\bullet}$ radicals in the discharge, with a much higher density for $OH^{\bullet}$ radicals than for $NO^{\bullet}$ [20]. The species formed in gliding arc discharge such as $OH^{\bullet}$ radicals are responsible for strong oxidizing effects whereas $NO^{\bullet}$ radicals for acidifying properties [21–23].

Photocatalysis of organic compounds using $TiO_2$ particles presents many advantages: the large number of organic compounds dissolved, or dispersed in water undergo complete mineralization. So $TiO_2$ has been extensively used in the mineralization of toxic organic contaminants present in wastewater. Hence, combined plasmachemical treatment and $TiO_2$-mediated heterogeneous process may be very efficient for both decolourization and degradation. Photodegradation processes proceed by different routes, involving for example electron transfer from the excited state of the dye molecules adsorbed on the $TiO_2$ surface into the conduction band of $TiO_2$. $TiO_2$ has an appropriate energetic separation between its valence band (VB) and conduction band (CB), which can be surpassed by the energy of a solar photon. The VB and CB energies of the $TiO_2$ are estimated to be +3.1 and −0.1 V, respectively, which mean that its band gap energy is 3.2 eV and it absorbs in the near UV light ($\lambda < 387$ nm). Such processes are less efficient than those occurring with UV light [24]. When aqueous $TiO_2$ suspension is irradiated with light energy greater than the band gap energy of the semiconductor, conduction band electrons ($e_{cb}{}^-$) and valence band holes ($h_{vb}{}^+$) are formed. The photogenerated electrons react with adsorbed molecular $O_2$, reducing it to superoxide radical anion $O_2{}^{\bullet -}$, and the photogenerated holes either can oxidise the organic molecules directly, or can oxidise $OH^-$ ions and water molecules adsorbed on the $TiO_2$ surface to $OH^{\bullet}$ radicals [25,26]. These will act as strong oxidizing agents that can easily attack any organic molecules adsorbed on, or located close to, the surface of the catalyst, thus leading to their complete degradation into small inorganic species. Reactions (1)–(5):

$$TiO_2 + h\upsilon \rightarrow TiO_2(e_{cb}{}^- + h_{vb}{}^+) \quad (1)$$

$$O_2 + e_{cb}{}^- \rightarrow O_2{}^{\bullet -} \quad (2)$$

$$H_2O + h_{vb}{}^+ \rightarrow OH^{\bullet} + H^+ \quad (3)$$

$$OH^{\bullet} + RH \rightarrow R^{\bullet} + H_2O \quad (4)$$

$$R^{\bullet} + O_2 \rightarrow R'COO^{\bullet} \rightarrow R'^{\bullet} + CO_2 \quad (5)$$

The aim of this work is to treat an anthraquinonic dye acid green 25 (AG 25) by coupling the gliding arc discharge with $TiO_2$ as photocatalyst thereby attempting to generate hydroxyl radical ($OH^{\bullet}$) reactive species from both humid air plasma and photocatalyst.

Anthraquinonic dyes represent the second most important class of commercial dyes after azo compounds and are mainly used for dyeing polyamides, leather and wool [27]).

## 2. Experimental

### 2.1. Materials and reagents

Anthraquinonic acid green 25 ($C_{28}H_{22}N_2O_8S_2{\cdot}2Na$) or toluennesulfonic acid, 6,6′-(1,4-anthraquinonylenemino) disodium salt, a commercial product purchased from Agros Organic was used as received. The chemical structure and absorption spectra of AG 25 are shown in Fig. 1. The photocatalyst $TiO_2$ was obtained from Merck (anatase as major component), with a specific surface area of 11 $m^2\ g^{-1}$. All other chemicals were of analytical reagent grade. The natural pH of the aqueous dye solution is 5.1. Distilled water was used to make the dye solutions of desired concentration.

### 2.2. Apparatus

The gliding arc system used for this study was described elsewhere [28] and various devices were tested for pollution abatement of liquid effluents (Fig. 2). An electric arc forms between two diverging electrodes raised to a convenient voltage difference at the minimum gap. A special transformer (9000 V; 100 mA without charge) provides the electric power. The arc is pushed away from the ignition point by the feeding gas flow and sweeps along the maximum length of the electrode gap and forming a large plasma plume. A new arc then appears and develops according to the same procedure. The plasma plume is disposed close enough to the liquid target, so that it licks the liquid surface, and allows the chemical reactions to take place at the plasma–solution interface (Reactions (6)–(16)).

The diffusion process in the liquid is improved by conversion in the liquid phase due to the airflow and magnetic stirring. The resulting plasma is actually quenched plasma at atmospheric pressure and quasi-ambient temperature.

$$H_2O + e^- \rightarrow H^{\bullet} + OH^{\bullet} + e^- \quad (6)$$

$$O_2 + e^- \rightarrow O(^3P) + O(^1D) + e^- \quad (7)$$

$$N_2 + e^- \rightarrow N(^4S) + N(^2D) + e^- \quad (8)$$

$$N(^2D) + O_2 \rightarrow NO^{\bullet} + O \quad (9)$$

$$H^{\bullet} + O_2 \rightarrow HO_2{}^{\bullet} \quad (10)$$

$$HO_2{}^{\bullet} + NO^{\bullet} \rightarrow NO_2 + HO^{\bullet} \quad (11)$$

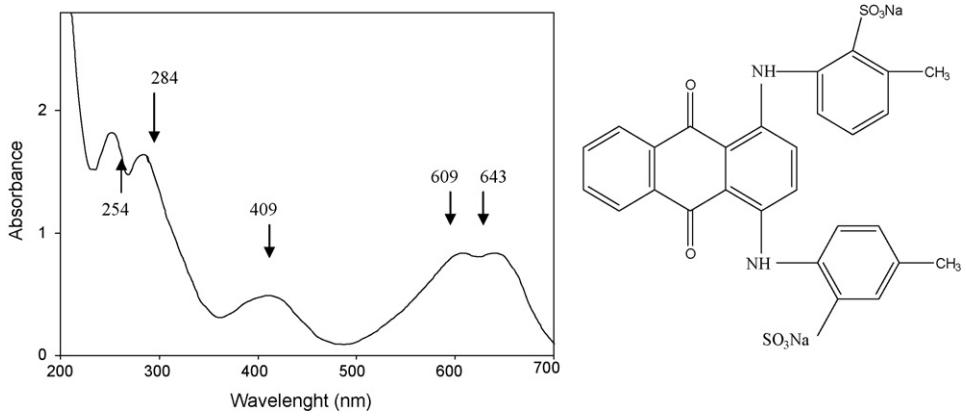


Fig. 1. UV–vis absorption spectra and the structure of AG 25 dye.

$$NO_2 + HO^{\bullet} \rightarrow H^+ + NO_3^- \quad (12)$$

$$NO^{\bullet} + HO^{\bullet} \rightarrow HNO_2 \quad (13)$$

$$HNO_2 \Leftrightarrow H^+ + NO_2^- \quad (14)$$

$$NO^{\bullet} + O(^3P) \rightarrow NO_2 \quad (15)$$

$$O_2 + O(^3P) \rightarrow O_3 \quad (16)$$

The treatment was carried out for different plasma-exposure times. The working parameters were identified as the electrode gap $e$ (3 mm), the distance $d$ (5 cm) between the electrode neck and the liquid surface, the gas flow rate $Q$ (800 L $h^{-1}$), and the nozzle diameter Ø (1 mm) which delivers a cylindrical gas flow.

### 2.3. Procedure and analytical methods

A volume of 180 mL of different AG 25 aqueous solutions (80, 160 and 240 μM) was introduced in the reactor. The treatment of the dye solution was investigated as a function of plasma-exposure time $t$ (1, 5, 10, 15, 30, 45, 60, 75, 90, 120, 150 and 180 min). The solutions were used without and with $TiO_2$ (at 0.5, 1, 1.5, 2, 2.5 and 3 g $L^{-1}$ concentration) with an aim of optimising the quantity of catalyst to use in the target solution. The suspension was stirred for 30 min in the dark to attain adsorption equilibrium between the dye solution and the $TiO_2$ surface. Before analysis, aliquots of the aqueous suspensions were collected at selected treatment time intervals, centrifuged and filtered trough 0.45 μm Millipore filters to remove catalyst $TiO_2$ particles.

UV–vis analyses of the AG 25 solutions during the treatment (from 0 to 180 min) were carried out in the 200–700 nm wavelength range on a UV–vis Optizen 2021 double beam spectrophotometer to follow decolourization versus plasma-treatment time. The concentration of AG 25 for every treated sample was determined by spectrophotometry at $\lambda_{max}$ = 643 nm. The degradation was determined from the chemical oxygen demand (COD); COD measurements were performed by titration according to the NF T 90–101 AFNOR standard procedure. Analysis of sulphate ions was carried out using colorimetric methods following the AFNOR standard procedure.

## 3. Results and discussion

### 3.1. Plasmachemical treatment without $TiO_2$

#### 3.1.1. Study of decolourization

Fig. 3 shows the UV–vis spectra of the AG 25 solution (80 μM) for 1, 5, 10, 15, 30, 45, 60, 75, 90, 120, 150 and 180 min of plasmachemical treatment. The spectrum corresponding

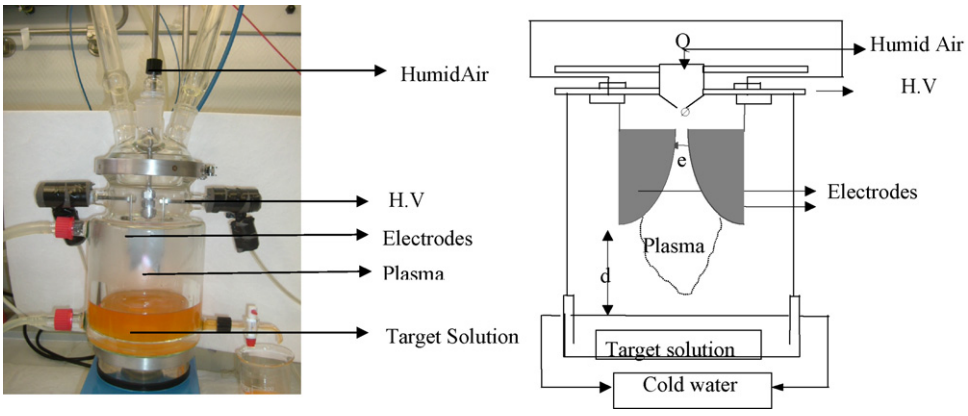


Fig. 2. Experimental set-up of the gliding arc plasma.

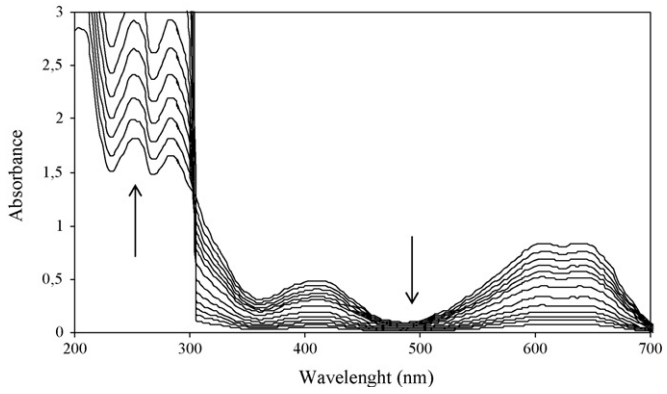


Fig. 3. UV–vis spectra of AG 25 as a function of plasma treatment time.

to the untreated sample (Fig. 1) is characterized by a double band in the visible region whose maximum absorbance corresponds to 609 and 643 nm and a band located at 409 nm characterizing AG 25. The bands in the ultraviolet region are, respectively, localized at 254 and 284 nm and are attributed to the benzene cycles substituted by $SO_3^{2-}$ groups and to the anthraquinonic part.

The plasmachemical treatment of the AG 25 aqueous solution caused a reduction of the absorbance in the visible part of the spectrum, whereas at short wavelengths some peaks attributed to benzene appear multi-substituted [29]. Progressive decolourization was total after 180 min of treatment (Fig. 3). Decolourizing was observed during the very first minutes of treatment. Indeed, the evolution of the residual concentration versus time (Fig. 4), takes an exponential form. Decolourization was fast during the first 30 min of treatment since the concentration of the dye decreased from 80 to 20 μM at a rate of 75.5%. Beyond this time, decolourization decreased slowly to reach 84.4, 91.4 and 100% in 60, 120 and 180 min, respectively.

The quantitative interpretation of the results requires a kinetic model (Eq. (17)). The decolourization reactions follow pseudo-first order kinetics:

$$\frac{-\,\mathrm{dC}}{\mathrm{d}t} = kt \tag{17}$$

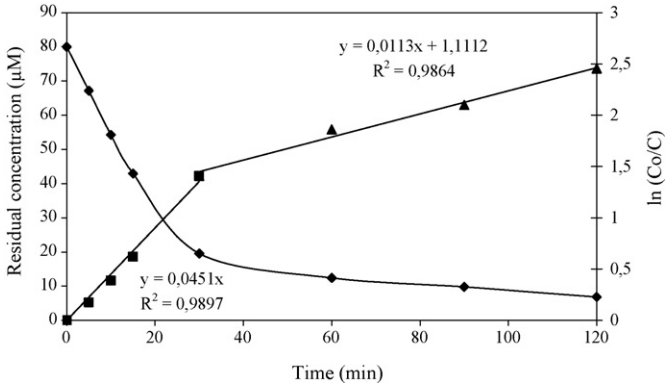


Fig. 4. Evolution of the residual concentration and decolourization kinetics of AG 25.

where $k$ is pseudo-first order constant rate, $t$ the treatment time and $C$ is dye concentration at time $t$. Integrating this equation for the boundary conditions $C = C_0$ at $t = 0$ and $C = C$ at $t = t$ leads to the following equation:

$$\ln\left(\frac{C_0}{C}\right) = kt \tag{18}$$

The kinetics of decolourization of AG 25 represented by $\ln(C_0/C) = f$ (time) (Fig. 4) based on the disappearance of the visible band located at 643 nm indicates that the reaction comprises two successive first order kinetics steps. The treatment of the initial solution, strongly coloured, follows fast decolourization kinetics with a rate constant of 0.045 $\mathrm{min}^{-1}$ owing to a significant flow of hydroxyl radicals occurring at the beginning of the electrical discharge [21]. Beyond 30 min of treatment, a second step with a rate constant of 0.0113 $\mathrm{min}^{-1}$ is observed.

### 3.1.2. Study of degradation

Degradation was followed by COD determination, which reflects the degree of mineralization [21,30]. Complete oxidation of AG 25 (Eq. (19)) may be written as follows:

$$C_{28}H_{22}N_2O_8S_2Na_2 + 35O_2 \rightarrow 28CO_2 + 2NO_3^- + 4H^+ + 2SO_4^{2-} + 2Na^+ + 8H_2O \tag{19}$$

Calculation of the theoretical initial COD (89.6 mg $L^{-1}$ $O_2$.), was compared with that obtained experimentally (88.1 mg $L^{-1}$ $O_2$) to determine the accuracy of the analytical method used. The kinetics of COD removal depicted in Fig. 5 indicates a fall of the COD from 88.1 to 70.4 mg $L^{-1}$ $O_2$ after 15 min of treatment, which represents an abatement of 20%. COD abatement attained 50% after 1 h of treatment and 84.6% at the end of 3 h of treatment.

The study of $\ln(\mathrm{COD}_0/\mathrm{COD})$ versus time (Fig. 5) shows that degradation follows pseudo-first order kinetics with a constant rate of 0.0103 $\mathrm{min}^{-1}$.

### 3.1.3. Correlation between decolourization and degradation

Decolourization results from the destruction of the chromophoric group characterized by $\lambda_{max}$ (609 and 643 nm)

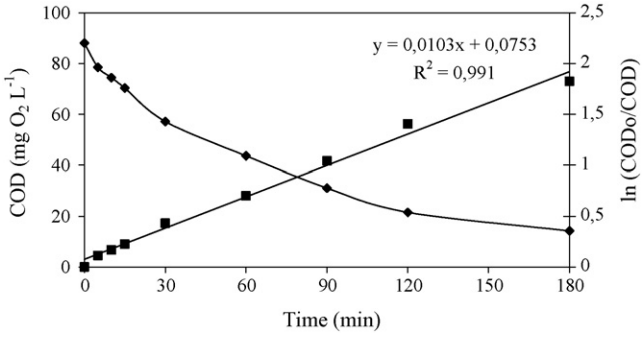


Fig. 5. Evolution of the COD and kinetics of degradation of AG 25: (◆) COD; (■) $\ln(\mathrm{COD}_0/\mathrm{COD})$.

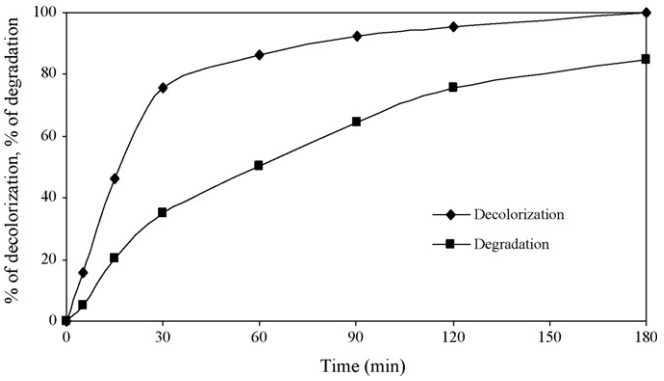


Fig. 6. Decolourization and degradation of AG 25.

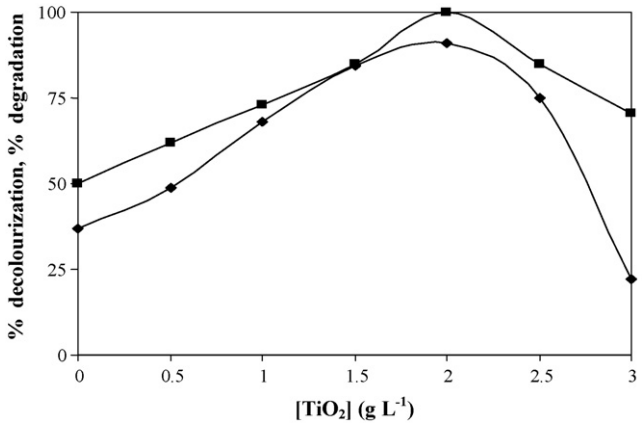


Fig. 7. Percent decolourization (15 min treatment time) and degradation (1 h treatment time) vs. $TiO_2$: (◆) degradation; (■) decoulorization.

while degradation concerns bond breaking in the aromatic part of dye (C–C; C=C; C–N, C–S; C=N). Fig. 6 shows simultaneously the rate of decolourization and the residual COD. The comparison of decolourization and degradation during the first half hour of treatment shows the faster decolourization rate at the expense of degradation. Beyond this time, this phenomenon was inverted, since degradation was faster than decolourization.

The difficulty in degrading AG 25 was primarily due to the different affinity of the plasma-producing species for the different parts of the dye molecule. Indeed the OH( radicals attack initially the chromophoric group (at 643 nm) and the fragile group, N–H thereby causing strong decolourization. Further degradation occurs because of the increased availability of the oxidizing species [29,31].

### 3.2. Plasmacatalysis: treatment with $TiO_2$

The coupling of the non-thermal plasma of glidarc type with $TiO_2$ in aqueous solution for depollution purposes was studied for the first time in this work. It aimed at improving the effectiveness of the treatment and to generalize it to other treatments. The treatment in the presence of catalyst must take account of several parameters such as the optimal quantity of catalyst to use, the pH of the solution, the nature of the substance to be treated, the temperature as well as the compounds present in the solution. Consequently, the optimal concentration of catalyst will depend on the pollutant nature and on the reactive species formed during the treatment. Increasing the dose of $TiO_2$ to be used in the target solution will entail a limiting effect (screening effect) which is due to the excess of the particles preventing the light from exciting the surface of the photocatalyst [29]. All the experiments involving the catalyst were initially agitated in the dark during 30 min for the dye to attain adsorption equilibrium on the particles surface and to ensure reproducibility of the results.

#### 3.2.1. Determination of the optimal concentration of $TiO_2$

The determination of the optimal concentration of catalyst was made regarding decolourization and degradation of the AG 25 dye as a function of time. We varied the catalyst concentration from 0.5 to 3 g $L^{-1}$.The results show that decolourization and degradation increased with treatment time until 2 g $L^{-1}$ (Fig. 7). Complete decolourization was obtained within 15 min but the maximum of degradation (84%) was attained within 1 h of treatment time. Beyond this optimal catalyst concentration, a reduction in the treatment efficiency was observed.

These results show that for any concentration higher than 2 g $L^{-1}$, other factors can affect degradation. Thus, for increased $TiO_2$ concentrations, aggregation of the particles reduces the contact surface between the solution and catalyst, decreases the number of active sites on the surface rendering difficult light infiltration resulting in a loss of catalyst efficiency.

#### 3.2.2. Study of decolourization

The treatment of an 80 μM AG 25 solution in the presence of $TiO_2$ caused the reduction in the absorbance corresponding to the characteristic wavelengths (254, 284, 409, 609 and 643 nm). The absorption bands decrease with catalyst concentration (0, 0.5, 1, 1.5 and 2 g $L^{-1}$). Fig. 8 represents the spectra corresponding to the treatment of AG 25 during

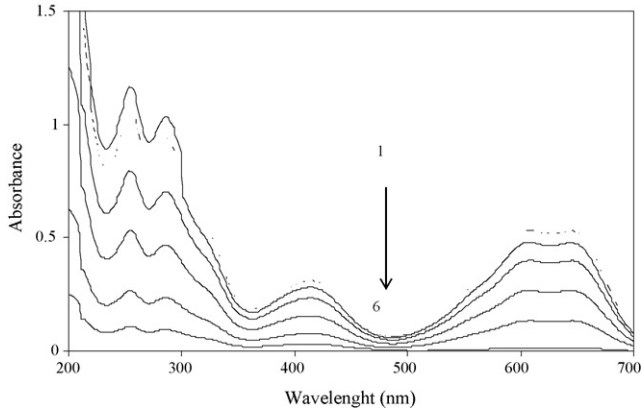


Fig. 8. UV–vis spectra vs. $TiO_2$ concentration for a 15 min plasmachemical trearment time: (1) untreated (2) 0 g $L^{-1}$, (3) 0.5 g $L^{-1}$, (4) 1 g $L^{-1}$, (5) 1.5 g $L^{-1}$ and (6) 2 g $L^{-1}$.

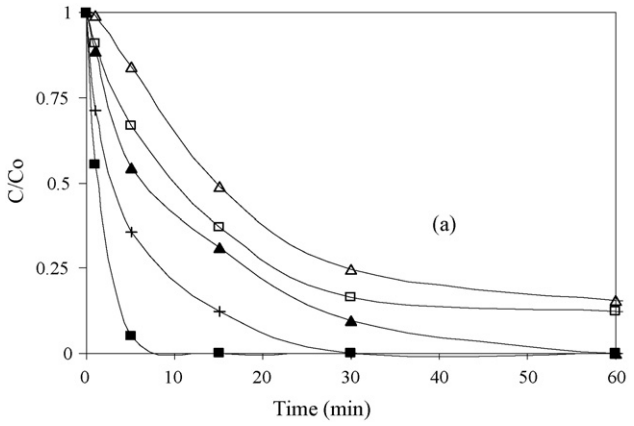


Fig. 9. AG 25 (80 μM) depletion as a function of treatment time in the presence of $TiO_2$: (■) 2 g $L^{-1}$; (+) 1.5 g $L^{-1}$; (▲) 1 g $L^{-1}$; (□) 0.5 g $L^{-1}$; (△) 0 g $L^{-1}$.

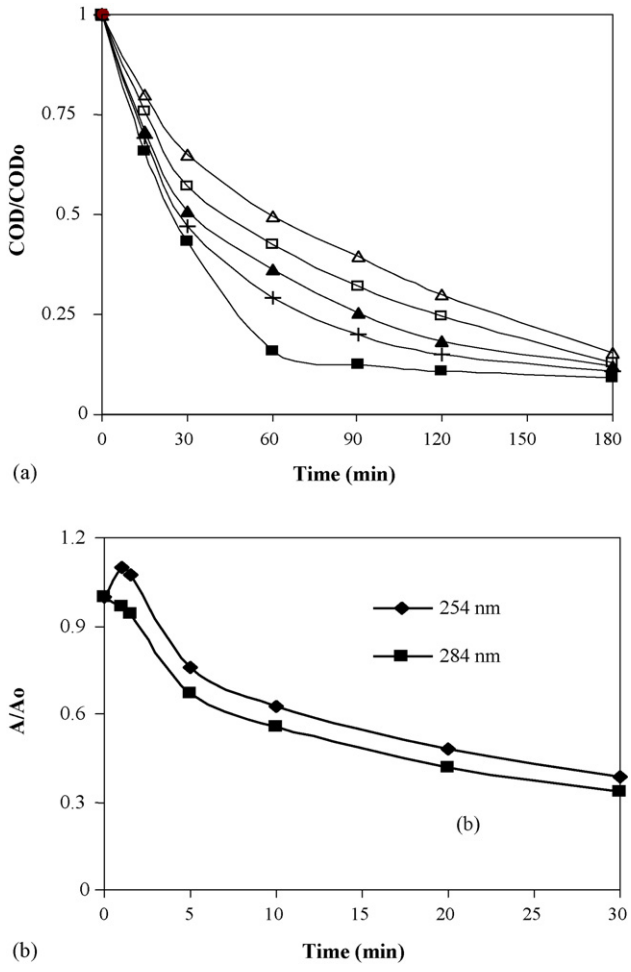


Fig. 10. (a) Reduced COD of AG 25 (80 μM) with amount of $TiO_2$: (■) 2 g $L^{-1}$; (+) 1.5 g $L^{-1}$; (▲) 1 g $L^{-1}$; (□) 0.5 g $L^{-1}$; (△) 0 g $L^{-1}$and (b) reduced AG 25 absorbance (80 μM) at 2 g $L^{-1}$ $TiO_2$ concentration.

15 min. This time was sufficient for a total decolourization of the dye solution.

The presence of catalyst clearly improves the plasma-producing treatment, because a significant variation in the spectra, whose band intensity decreases according to the amount of $TiO_2$, was observed. Nevertheless, beyond a 2 g $L^{-1}$ $TiO_2$ concentration, a turbid solution was observed causing an absorbance increase. UV–vis spectra obtained in the presence and the absence of $TiO_2$, showed that the reduction in absorbance was not only significant in the presence of catalyst but it concerned both spectrum ranges (visible and ultraviolet) as well. No new band appeared during this treatment, unlike the treatment without catalyst where the absorbance increased at small wavelengths. This result shows that when only the plasmachemical treatment was involved, light intermediate products were progressively formed during treatment characterized by an increase in the absorbance at small wavelengths. On the other hand, in plasmacatalysis, these same products disappear as a function of treatment time with the reduction of the corresponding absorbances. Fig. 9 represents the reduced concentration $C/C_0$ of AG 25 (80 μM) in the presence of the varying $TiO_2$ concentration. The results show the progressive decolourizing with catalyst concentration. Total decolourization was obtained within 15 min of treatment and for a 2 g $L^{-1}$ $TiO_2$ concentration.

The plasmachemical treatment (without catalyst) gave 46.51% AG 25 decolourization during 15 min of treatment with pseudo first order kinetics and different rate constants. Plasmacatalysis gave a decolourization of 100% for the same time treatment. From the kinetic point of view, the reduction in the intermediate compounds made it possible to have a one-step decolourization kinetics representing a first order reaction.

### 3.2.3. Study of degradation

Fig. 10a shows the evolution of the reduced COD (COD/$COD_0$) of AG 25 (80 μM) as a function of time for various amounts of $TiO_2$.The plots in Fig. 10b represent the imprint of the aromatic part of the dye [34]. The evolution of the absorbance at 284 and 254 nm shows the disappearance of the anthraquinonic structure of AG 25. After 30 min of treatment time, the stabilization of certain AG 25 benzene cycles non-subject to plasmachemical treatment seems to occur. The curves obtained show that the COD decreases with the amount of $TiO_2$ added.

Thus, for a 60-min treatment time, the rate of degradation attained 84% in the presence of the optimal quantity of catalyst (2 g $L^{-1}$) and 91% for a 180-min treatment time. The residual COD was only 7 mg $L^{-1}$ $O_2$. The results obtained are summarized in Table 1.

The value of the COD was stabilized at 7 mg $L^{-1}$ $O_2$ accounting for the persistence of some aromatic compounds which represent the basic structures of AG 25.This is in agreement with the results by ref. [27] for the degradation of the AB 25 dye, which is an anthraquinonic compound whose structure is comparable to AG 25. Indeed, a 3-h photoctalytic treatment allowed total decolourization of the dye. Nevertheless, persistence of some aromatic cycles was observed. The UV–vis spectra obtained during the treatment without catalyst, showed a significant increase in the absorbance at small wavelengths, accounting for the formation of aromatic

Table 1
Degradation rate and kinetic constants for the plasmacatalytic treatment of AG 25

| $TiO_2$ concentration ($g\ L^{-1}$) | Degradation rate (%) | Rate constant ($mn^{-1}$) |
|---|---|---|
| 0 | 37.0 | 0.0103 |
| 0.5 | 48.7 | 0.0141 |
| 1 | 68.0 | 0.0179 |
| 1.5 | 84.3 | 0.0217 |
| 2 | 91.0 | 0.0430 |
| 2.5 | 75.0 | 0.0210 |
| 3 | 19.5 | 0.0011 |

compounds lighter and less conjugated than the initial molecule. The catalytic effect generated a decrease in intermediate compounds, which disappeared with treatment time. This can be explained by a possible adsorption of the intermediate products on the surface of catalyst. In effect, Fig. 10b shows that the aromatic species whose absorbance is at 254 nm was produced in significant amount during the first 2 min of the plasmacatalytic treatment then decreased quickly. This can be explained by its migration towards the catalyst. This study confirms that the aromatic compounds formed during the plasmachemical treatment remain in solution, but are adsorbed on $TiO_2$ surface during the plasmacatalytic treatment.

The appearance of the sulphate ions is another proof of the mineralization of AG 25 during the treatment. Indeed, dyes containing sulphur atoms in the form of sulphonate can be mineralized into sulphate ions by the attack of hydroxyl radicals. The attack of $R–SO_3^{2-}$ by OH radical is favoured if the molecule, via its orientation on the surface of $TiO_2$, is adsorbed via this group [32–34] according to the following mechanism (Eqs. (20)–(24)):

(a) Photo-mediated hydrolysis:

$$R - SO_3^- + H_2O \rightarrow RH + HSO_4^- \quad (20)$$

$$HSO_4^- \Leftrightarrow SO_4^{--} + H^+ \quad (21)$$

(b) Catalyst photo-activation:

$$TiO_2 + h\upsilon \rightarrow e^- + h^+ \quad (22)$$

$$H_2O + h^+ \rightarrow OH^\bullet + H^+ \quad (23)$$

(c) $OH^\bullet$ attack:

$$R - SO_3^- + OH^\bullet \rightarrow R^\bullet + H^+ + SO_4^{2-} \quad (24)$$

The calculated final concentration of sulphates at the end of the treatment was 15.36 mg $L^{-1}$. We found 12.95 mg $L^{-1}$, i.e., approximately 83%. This can be explained by the adsorption of the sulphates on the catalyst, especially in acid solution. The decrease in the pH favours the formation of $Ti - OH_2^+$ groups, which tend to attract sulphate ions and retain them on the surface of the catalyst. Fig. 11 shows the evolution of sulphate ion concentration during the treatment of AG 25 in the presence of the catalyst. Sulphate ion formation versus treatment time was studied for plasmachemical treatment. The values obtained

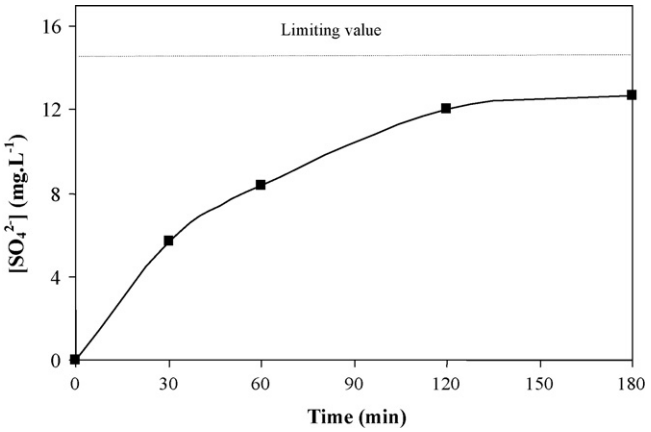


Fig. 11. Variation of sulphate ion concentration versus plasmacatalytic treatment time of AG 25 dye (80 μM).

for sulphates were too low to be detected by the nephelometric method, despite a relatively high degradation rate.

The treatment by plasma in humid air has also an acidifying effect. As a result, the pH of the dye solution passed from 5.1 to 0.91 after a 180 min treatment time. The acidification is very rapid since in less than 5 min of treatment time, the pH dropped to 3.2. The addition of $TiO_2$ caused a more marked pH decrease compared to the treatment in the absence of the catalyst (Table 2).

According to the values obtained, the treatment in the presence of $TiO_2$, further acidifies the treated solution as can be seen from reaction (25). The effect of the pH on the photocatalytic oxidation is well known. The variation of the pH influences the adsorption of the molecules of the dye on the surface of $TiO_2$ [33]. The photocatalytic activity of $TiO_2$ depends on its acido-basic properties. The surface of $TiO_2$ is positively charged in acid medium and thus attracts the dye through its negatively charged sulphonic groups. Consequently, the acidity of the solution favours the formation of the OH hydroxyl radicals obtained from the positive holes ($H^+$) according to the reaction (Table 3):

$$H_2O \Leftrightarrow H^+ + OH^- + h^+ \rightarrow OH^\bullet + H^+ \quad (25)$$

### 3.2.4. Correlation between decolourization and degradation

During the plasmachemical treatment, we noted a close relationship between decolourization and degradation. This

Table 2
Influence of $TiO_2$ concentration on the final pH (180 min)

| $TiO_2$ concentration ($g\ L^{-1}$) | $pH_{final}$ |
|---|---|
| 0.0 | 1.70 |
| 0.5 | 1.13 |
| 1.0 | 1.09 |
| 1.5 | 1.01 |
| 2.0 | 0.91 |
| 2.5 | 0.84 |
| 3.0 | 0.84 |

Table 3
Decolourization and degradation rate constants for plasmachemical and plasmacatalytic treatment

| AG 25 concentration (μM) | $10^3 \times K_{DEC}$ ($min^{-1}$) with $TiO_2$ | $10^3 \times K_{DEC}$ ($min^{-1}$) without $TiO_2$ | $10^3 \times K_{DEG}$ ($min^{-1}$) with $TiO_2$ | $10^3 \times K_{DEG}$ ($min^{-1}$) without $TiO_2$ |
|---|---|---|---|---|
| 80 | 455.0 | 45.0 | 43.0 | 10.3 |
| 160 | 183.0 | 15.5 | 12.8 | 7.0 |
| 240 | 132.0 | 14.9 | 7.7 | 4.9 |

correlation was also found in the plasmacatalytic treatment (Fig. 12).

The decolourization of the solution at the beginning of the treatment exhibited very fast kinetics, whereas the degradation evaluated by the residual COD was relatively slow. After a 15 min treatment time, the solution was completely decolourized. This phenomenon can be explained by the fact that the reactive species generated by plasma, will at this stage target degradation since decolourization being maximum will not further consume the OH radicals. The same phenomenon was observed in the treatment in the absence of catalyst. During treatment without catalyst, this time was 30 min, in the presence of $TiO_2$, it decreased to 15 min for complete decolourization, inducing significant degradation. The kinetics of degradation during the first minutes of treatment was slower than that of decolourization. The intermediate products formed will compete with the initial dye molecules with respect to the OH radicals responsible for oxidation [35,36]. The degradation rate decrease could be related to the difficulty in converting the atoms of nitrogen and sulphur into oxidized compounds. The degradation follows pseudo first order kinetics with rate constant equal to 0.043 $min^{-1}$, hence a value four times higher than that obtained in the treatment without catalyst (0.0103 $min^{-1}$).

### 3.2.5. Effect of initial dye concentration

As aforementioned, the concentration plays a significant role in pollutants treatment since they can occur at high concentrations in industrial effluents. The same concentrations were selected as in the treatment without catalyst (80, 160 and 240 μM). The concentration of $TiO_2$ was maintained at 2 g $L^{-1}$.The increase in the initial dye concentration resulted in a reduction in the elimination rate. These results corroborate those cited in ref. [37]. Increasing AG 25 concentration from 80 to 240 μM, resulted in a decolourization percent decrease from 93.9 to 75.9% for a treatment time of 10 min and a degradation percent decrease from 56.9 to 20.4% for a 30-min treatment time. We noted a reduction in the plasmacatalytic efficiency for the treatment of more concentrated AG 25 dye solutions. This is due to the increase in the amount of the dye adsorbed on the surface of the catalyst which will inhibit the activity of the OH

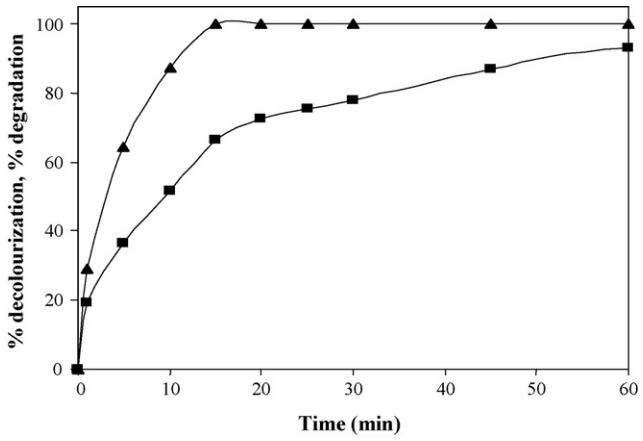


Fig. 12. Plasmadecolourization and plasmadegradation of AG 25 dye (80 μM): (▲) decolourization; (■) degradation.

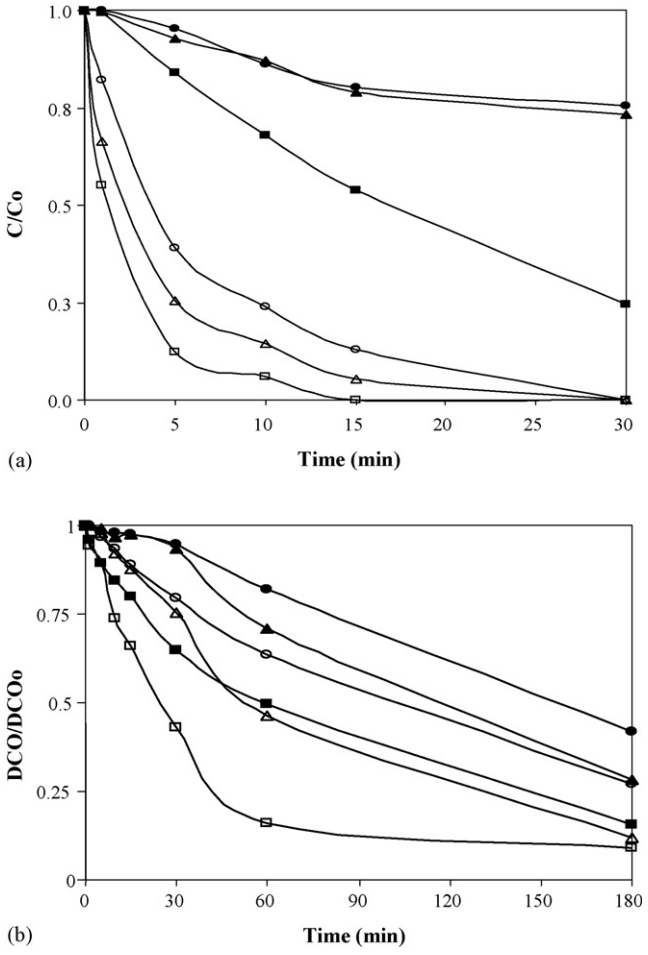


Fig. 13. Effect of initial AG 25 concentration in the presence of 2 g $L^{-1}$ de $TiO_2$: (a) reduced concentration evolution; (b) reduced COD evolution. (■) 80 μM plasmachemistry; (□) 80 μm plasmacatalysis; (▲) 160 μM plasmachemistry; (△) 160 μM plasmacatalysis; (●) 240 μM plasmachemistry; (○) 240 μM plasmacatalysis.

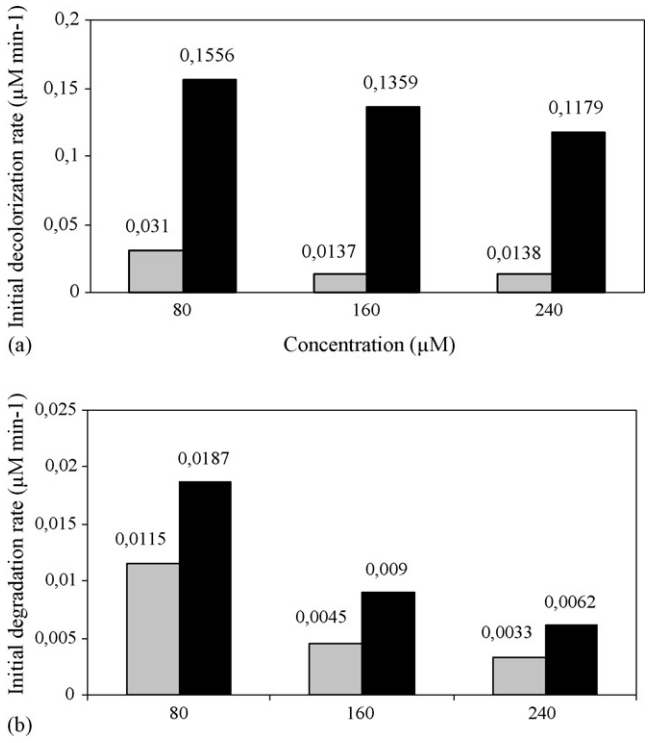


Fig. 14. Initial AG 25 (a) decolourization rate for three concentrations of AG 25; (b) degradation rate for three concentrations of AG 25. (□) Plasmachemistry; (■) plasmacatalysis.

radicals, in addition to the more intense colouration preventing the light from infiltrating into the medium. For these high concentrations, UV radiations can be stopped by the dye molecules thereby affecting the photocatalytic process [38]. The reduced concentration and chemical oxygen demand for the three concentrations studied for both treatment types are depicted in Fig. 13. As expected, the plasmacatalytic treatment is clearly more efficient than the plasmachemical one.

Effectively, the increase in the initial concentration of AG 25 decreases the rate of decolourization in plasmachemical treatment. Indeed, a rate of 84.4% was obtained for an initial concentration of 80 μM after 1 h of treatment; it was 46.5% for a 160 μM solution and only 27.3% for a 240 μM solution. In addition, degradation decreased in an identical way and the results show that for a-1 h treatment time, the degradation rate was 50.4% for the 80 μM solution, 29.2% for the 160 μM solution and 18.1% for the 240 μM.

The reaction rate constants obtained during the first 15 min of plasmachemical treatment, indicate that decolourization and degradation of AG 25 were faster for the small concentration (80 μM).

This behaviour can be explained by the non-availability of the plasma-producing species in a very coloured and opaque aqueous solution. Indeed, a more concentrated solution requires a more significant gas flow in order to produce more $OH^{\bullet}$ radicals and to increase the intermolecular distances of the dye [32].

From the output and reaction speed point of view, decolourization (Fig. 13a) and degradation (Fig. 13b) are definitely more significant for plasma treatment in the presence of catalyst. Consequently, one-step reactions with exponential type curves for treatments with $TiO_2$ were obtained, whereas without catalyst two-step reactions were involved, which can be explained by the availability of the $OH^{\bullet}$ radicals during the plasmacatalytic treatment and the contact homogeneity with the catalyst contact surface.

The efficiency of the plasmacatalytic treatment compared to the plasmachemical one is reflected in the rate constants values. Fig. 14(a and b) summarizes the results for both treatments. Higher initial decolourization and degradation rates in plasmacatalysis than those obtained by plasmachemistry were obtained. The plasma AG 25 elimination is connected to the concentration of both $^{\bullet}OH$ radicals and dye and it cannot to be associated to a first order kinetic. Consequently, the comparison between the different studies will be done using the initial degradation rate (mol $L^{-1}$ $min^{-1}$) rather than a pseudo first order kinetic constant.

## 4. Conclusion

The glidarc is a non-thermal source of plasma, which generates very reactive species such as OH radicals. These species exhibit powerful oxidizing properties capable of mineralizing organic compounds. In this study, we used the plasma in humid air for the degradation of the anthraquinonic AG 25 dye. Complete decolourization of the AG 25 solution was obtained after a 180-min plasma treatment time without catalyst, but for the $TiO_2$-mediated process, the treatment time was reduced to 15 min. The rate of degradation attained 50% for a 1-h plasma exposure time while for the $TiO_2$-assisted system, this rate increased to 84%. UV–vis spectrophotometry highlighted the decolourization of the AG 25, namely the destruction of the chromophores, whereas the abatement of the chemical oxygen demand confirmed degradation. The kinetic studies showed the faster decolourization rate compared to degradation. The use of the catalyst $TiO_2$ improved decolourization, just as degradation, occurring at a faster rate than in the $TiO_2$-free case. Reaction speeds as well as mineralization of the dye were significantly higher in the presence of $TiO_2$. Mineralization was attested by the high percentage of sulphate ions formed during the treatment. The rates of decolourization and degradation were maximum for an optimal amount of $TiO_2$ equal to 2 g $L^{-1}$, beyond which, the plasma/$TiO_2$ system was less effective. The initial dye concentration is a significant parameter as the treatment is better adapted to low concentrations. The combined plasma-$TiO_2$ method is a rapid and cost-effective means, which might prove well adapted to the removal of organic pollutants.

## References

[1] V.M. Correia, T. Stephenson, S.J. Judd, Environ. Technol. 15 (1994) 917–919.
[2] S. Dai, W. Song, T.Y. Zhuang, Adv. Tech. Semin. 4 (1996) 1–9.
[3] S.Y. Dai, W. Zhuang, Y. Chen, L. Chen, Environ. Chem. 14 (1995) 354–367.
[4] S. Kacha, M.S. Ouali, S. Elmaleh, Rev. Sci. de l'Eau. 10 (1997) 233–248.

[5] N. Lahav, U. Shani, J. Shabtai, Clays Miner. 26 (1978) 107–115.
[6] A.T. Sugiarto, S. Ito, T. Ohshima, M. Sato, J. Skalny, J. Electrostat. 58 (2003) 135–145.
[7] I. Arslan, I.A. Balciogul, D.W. Bahnemann, Dyes Pigments 47 (2000) 207–218.
[8] S0. Nam, V. Renganathan, P.G. Tratnyek, Chemosphere 45 (2001) 59–65.
[9] S. Sakthivel, B. Neppolian, M.V. Shankar, B. Arabindoo, M. Palachamy, V. Murugesan, Solar Energy Mater. Solar Cells 77 (2003) 65–82.
[10] W. Kan, Z. Jianying, L. Liping, Y. Shiying, C. Yingxu, J. Photochem. Photobiol. A 165 (2004) 201–207.
[11] A.G. Rincon, C. Pulgarin, Appl. Catal. B. 51 (2004) 283–302.
[12] P. Pichat, S. Vannier, J. Dussaud, J.P. Rubis, Solar Energy 77 (2004) 533–542.
[13] I.K. Konstantinou, A.A. Triantafyllos, Appl. Catal B 49 (2004) 1–14.
[14] C. Guillard, H. Lachheb, A. Houas, J. Photochem. Photobiol. A 158 (2003) 27–36.
[15] J. Bandara, C. Morrison, J. Kiwi, J. Photochem. Photobiol. A 99 (1999) 57–66.
[16] J. Cao, L. Wei, Q. Huang, S. Han, Chemosphere 38 (1999) 565–571.
[17] E. Guivarch, S. Trevin, C. lahitte, Environ. Chem. Lett. 1 (2003) 38–44.
[18] F. Abdelmalek, S. Gharbi, B. Benstaali, A. Addou, J.L. Brisset, Water Res. 38 (2004) 2338–2346.
[19] F. Abdelmalek, M.R. Ghezzar, M. Belhadj, A. Addou, J.L. Brisset, Ind. Eng. Chem. Res 45 (2006) 23–29.
[20] B. Benstaali, P. Boubert, G. Cheron, A. Addou, J.L. Brisset, Plasma Chem. Plasma Process. 22 (2002) 553–571.
[21] F. Abdelmalek, B. Benstaali, J.L. Brisset, A. Addou, Oriental J. Chem. 21 (2005) 21–24.
[22] D. Moussa, F. Abdelmalek, B. Benstaali, A. Addou, A.E. Hnatiuc, J.L. Brisset, Eur. Phys. J. Appl. Phys. 29 (2002) 189–199.
[23] K. Marouf-Khelifa, F. Abdelmalek, A. Khelifa, M. Belhadj, A. Addou, J.L Brisset, Sep. Purif. Technol., in press.
[24] M. Karkmaz, E. Puzenat, C. Guillard, J.M. Herrmann, Appl. Catal. B 51 (2004) 183–194.
[25] C.M. So, M.Y. Cheng, J.C. Yu, P.K. Wong, Chemosphere 46 (2002) 905–912.
[26] R.J. Davis, J.L. Gainer, G. O'Neal, I. Wu, Water Eviron. Res. 66 (1994) 50–53.
[27] I. Bouzaida, C. Ferronato, J.M. Chovelon, M.E. Rammahb, J.M. Herrmann, J. Photochem. Photobiol. A 168 (2004) 23–30.
[28] H. Lesueur, A. Czernichowski, J. Chapelle, French Patent 2,639,172 (1988).
[29] N. Daneshvar, D. Salari, A.R. Khataee, Chemosphere 48 (2002) 393–399.
[30] J.H. Yan, C.M. Du, X.D. Li, X.D. Sun, M.J. Ni, K.F. Cen, B. Cheron, Plasma Sources Sci. Technol. 14 (2005) 637–644.
[31] R. Comparelli, E. Fanizza, M.L. Curri, P.D. Cozzoli, G. Mascolo, A. Agostiano, Appl. Catal. B 60 (2005) 1–11.
[32] M. Stylidi, D.I. Kondarides, X.E. Verykios, Appl. Catal. B 47 (2004) 189–201.
[33] J. Fernandez, J. Kiwi, J. Freer, C. Lizama, H.D. Mansilla, Appl. Catal. B 48 (2004) 205–211.
[34] A.P. Toor, A. Verma, C.K. Jotshi, P.K. Bajpai, V. Singh, Dyes Pigments 68 (2006) 53–60.
[35] C. Hachem, F. Bocquillon, O. Zahraa, M. Bouchy, Dyes Pigments 49 (2001) 117–125.
[36] H. Lachheb, E. Puzenat, A. Houas, M. Ksibi, E. Elaoui, C. Guillard, J.M. Herrmann, Appl. Catal. B 39 (2002) 75–90.
[37] E. Kusvuran, O. Gulnaz, S. Irmak, M. Osman, M. Atanur, H. Ibrahim, H. Yavuz, O. Erbatur, J. Hazard. Mater. B 109 (2004) 85–93.
[38] M.H. Habibi, A. Hassanzadeh, S. Mahdavi, J. Photochem. Photobiol. A 172 (2005) 89–96.